Topic: TH/P3-17

Current Drive with Oscillating Magnetic Fields and Helicity Injection and Neutral Beam Injection in a D-He^3 FRC Reactor

R. Farengo, H. E. Ferrari, P. L. García Martínez
Centro Atómico Bariloche e Instituto Balseiro, 8400 Bariloche, RN, Argentina
E-mail:farengo@cab.cnea.gov.ar

R. A. Clemente
Instituto de Fisica Gleb Wataghin, UNICAMP, 13083-970 Campinas, SP, Brazil

Current drive with oscillating magnetic fields

We investigate the use of oscillating helical magnetic fields to sustain the toroidal and poloidal currents in a Reversed Field Pinch (RFP) [1]. This would allow continuous operation and eliminate the need for the internal dynamo, thus improving the confinement and the attractivness of the concept. Rotating magnetic fields (RMF) have been proved effective in sustaining field reversed configurations (FRCs) [2] and small spherical tokamaks [3]. In toroidal devices, where both poloidal and toroidal currents are necessary, a natural extension of the RMF technique is the double helix scheme. In this method, two sets of m=1 helical coils, wound around the plasma chamber and fed by strong rf sources with a phase difference of $\pi/2$, are employed.

Previous analysis of the double helix method showed that the efficiency is very low in tokamaks [4], where strong toroidal fields are present, but could be significantly higher in RFPs, which have smaller toroidal fields [5]. The physical model employed is the same as in [4]. It assumes fixed ions and uniform density and resistivity and employs a non linear Ohms law, without thermal effects, for the electrons. However, instead of looking for stationary solutions we solve the complete 2D time dependent equations that describe the penetration of the helical fields and the generation of the poloidal and toroidal currents.

We consider an infinite plasma column of radius a subject to the action of external traveling magnetic fields varying as $exp\{i(\theta+kz-\omega t)\}$, and a uniform static longitudinal magnetic field B_0. All lengths are normalized with a and the magnetic field with B_ω (amplitude of the helical field at the center of the column without plasma). Introducing helical coordinates, $x_1=r/a$, $x_2=\theta+kz$ and x_3 ignorable, the problem becomes 2D and we only need to calculate the third quasi-helical components of the dimensionless vector potential ($\hat{A}_3$) and magnetic field ($\hat{B}_3$). Knowing $\hat{A}_3$ and $\hat{B}_3$ we can obtain:

$$\hat{B}_1 = \frac{1}{x}\frac{\partial \hat{A}_3}{\partial x_2}\ ,\ \hat{B}_2 = -\frac{\partial \hat{A}_3}{\partial x}\ ,\ \hat{B}_\theta = \frac{\hat{B}_2 - hx\hat{B}_3}{1+h^2x^2}\ ,\ \hat{B}_z = \frac{\hat{B}_3 + hx\hat{B}_2}{1+h^2x^2}$$

The normalized equations depend on $\tau=\omega t$, h (pitch of the helical windings), $\hat{B}_0$ (external toroidal field), $\lambda^2 = a^2\mu_0\omega/2\eta$ and $\gamma = B_\omega / en\eta$ and are solved using a fourth order Runge-Kutta scheme. Outside the plasma $\hat{B}_3$ is uniform but can be time dependent and $\hat{A}_3$ is determined by the currents in the plasma and the coils, which are assumed to be very far from the plasma.

Two efficiencies $[\varepsilon_z = B_\theta(x=1); \varepsilon_\theta = B_z(x=1) - B_z(x=1)]$ and two synchronism parameteres $[\alpha_z = I_z / I_{z,\max}; \alpha_\theta = I_\theta / I_{\theta,\max}]$ are introduced for the axial (toroidal) and azimuthal (poloidal) driven currents respectively. The efficiencies measure how efficiently the externally produced field B_ω is employed to drive the currents while the synchronism parameters indicate how close we are to the maximum possible currents, which are obtained when all the electrons move with the traveling helical field.

Fig. 1 shows a plot of the steady-state efficiencies and synchronism parameters as a function of γ for $\lambda=20$, $h=1$ and $B_0=2$. It is clear that while boths efficiencies have a maximum around $\gamma=15.5$, the synchronism parameters increase with γ and become unity when γ is large enough. We note that since the ***cost*** of the method, in terms of the power needed to drive the current in the helical coils, increases with B_ω^2 it may not be feasible, or convenient, to increase B_ω (γ) to the level required for maximum current. Fig. 2 shows the steady-state magnetic field profiles (averaged over x_2) obtained with $\gamma=15.5$ and the other parameters as in Fig. 1, together with the values of the pinch parameters which are defined as:

$$F = \frac{\langle B_z(1)\rangle}{\overline{B}_z}, \quad \Theta = \frac{\langle B_\theta(1)\rangle}{\overline{B}_z}$$

Where $\langle..\rangle$ means average over x_2 and $\overline{B}_z$ is the volume average of B_z. It is clear that reasonable magnetic field profiles and pinch parameters close to the experimental values are obtained.

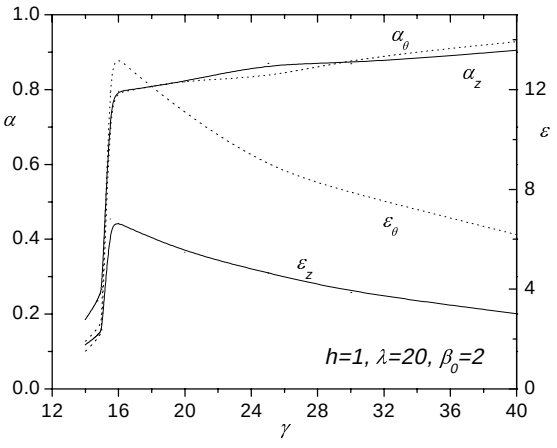

Fig. 1. Efficiencies and synchronism parameters as a function of γ

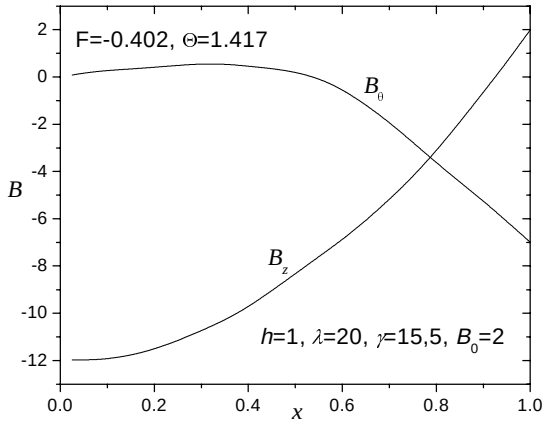

Fig. 2. Magnetic field profiles (normalized) and pinch parameteres

Table I shows the maximum efficiencies and the corresponding pinch parameters obtained for other values of λ and γ. In all cases the value of the external magnetic field was chosen to obtain pinch parameteres close to the experimental values. Note that for constant density, γ and λ increase with the temperature if classical resistivity is assumed.

λ	γ	$\hat{B}_0$	$\varepsilon_{z,max}$	$\varepsilon_{\theta,max}$	F	Θ
5	3.5	0.5	1.68	3.08	-0.426	1.442
10	6.5	1	3.91	7.86	-0.347	1.356
20	15.5	2	6.99	13.96	-0.402	1.417
30	26.0	3	9.08	18.42	-0.492	1.496

Table I. Maximum values of ε_z and ε_θ and pinch parameters for selected values of λ and $\hat{B}_0$.

Fig. 3 shows a plot of the toroidal and poloidal currents and the external magnetic field as a function of time for the same parameteres as in Fig. 1. The time required to reach a steady-state decreases with increasing γ.

The results show that it is possible to produce RFP like magnetic field profiles with pinch parameters close to the experimental values. The efficiencies obtained for moderate resistivity, and the observed scaling, indicate that this could be a very attractive method for high temperature plasmas.

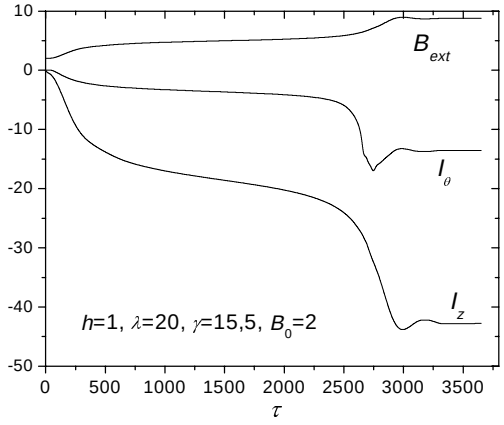

Fig. 3. Current and external field vs. time

We study the effect of finite electron inertia on rotating magnetic field (RMF) current drive in FRCs using a two fluid model [6]. The importance of inertial effects is measured by the ratio between the RMF frequency (ω) and the electron-ion collision frequency (ν). When ω/ν is very small, previous results corresponding to massless electrons are recovered.

Two situations are considered. The first one concerns the formation of a FRC by the RMF and the second the application of a RMF to an existing FRC, with fixed or rotating ions. Two different models are employed. In the first one (model I), the full radial and azimuthal dependence of the axial components of the magnetic field and vector potential are considered while in the second one (model II) only the averaged (over the azimuthal angle) value is included for the axial magnetic field. The results are analyzed by employing the efficiency (ε_θ) introduced above.

We find that electron inertial effects could be important, depending on the plasma and RMF parameters. When ω/ν increases, the maximum efficiency decreases and the value of γ required to obtain this maximum increases. In addition, the penetration time also increases. Since ν decreases with increasing temperature and decreasing density, these effects should become more important as fusion relevant temperatures are approached. Fig. 4, obtained with model I, shows the efficiency as a function of time for γ=5.75, λ=5 and different values of ω/ν while Fig. 5, obtained with model II, shows the steady-state efficiency as a function of γ for λ=50 and different values of ω/ν.

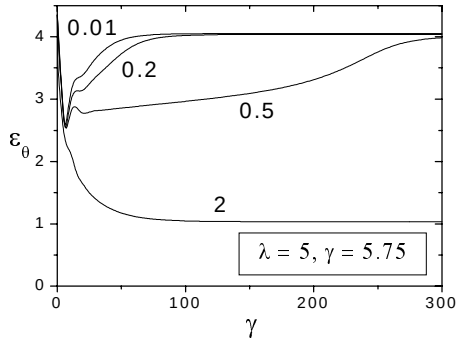

Fig. 4. Efficiency vs. time for different values of ω/ν.

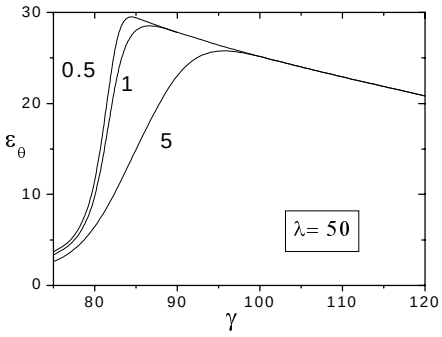

Fig. 5. Efficiency vs. γ for different values of ω/ν.

Neutral beam injection in a D-^{3}He Field Reversed Configuration reactor

Due to its high β ($\beta\approx1$) the Field Reversed Configuration (FRC) is ideally suited to burn advanced fuels. A conceptual design of a D-^{3}He FRC reactor partially sustained by neutral beam injection (NBI) was proposed by Momota et al. [7]. Here we employ the Monte Carlo code already used to study NBI into medium size FRCs [8] and Spheromaks [9] operating with D to study NBI in a FRC reactor with parameters similar to those quoted in the ARTEMIS [7] project. The code calculates the trajectories of individual particles integrating the equations of motion and including collisions. The exact orbits are calculated because the large Larmor radius of the energetic beam ions prevents the use of gyro-averaging.

The FRC plasma consists of D ions, ^{3}He ions and electrons, and it is assumed to be in MHD equilibrium. Since the required beam current (8 MA) is a small fraction of the total plasma current (200 MA) it is not necessary to calculate a self-consistent equilibrium (including the beam current). The equilibria are obtained by solving the Grad-Shafranov equation with the following functional dependence for the pressure:

$$p(\psi) = G_0\left[\frac{\psi}{\psi_0} - \frac{C}{2}\left(\frac{\psi}{\psi_0}\right)^2\right],$$

where G_0 is a constant, ψ_0 is the magnetic flux at the null and C is the "hollowness" parameter. When C>0 the equilibrium is hollow and when C<0 it is peaked. The

ARTEMIS design has a separatrix radius r_s=112 cm and a length $2z_s$=1700 cm. The beam is specified by indicating the energy of the neutral particles, the axial location where the beam is injected, the injection angle and the impact parameter (b).

Figures 6 and 7 show the spatial distribution of the beam current density and deposited power for a 5 A neutral beam injected at the midplane (z=0), with b=80 cm and perpendicular to the FRC axis. The equilibrium is peaked (C=-10) and the plasma parameteres are the similar to those used in [7], with the same external field and a somewhat lower density ($n_{e,\max}$=6.4×10^{14} cm^{-3}, T_e=T_D=T_{He}=87.5 keV, r_0≈80cm, E_{Beam}=1 MeV, B_{ext}=6.7 T, n_{He}=n_D/2). The total beam current obtained for this case is I_{Beam}= 0.48 MA, much lower than the value quoted in [7]. If a hollow equilibrium (C=0.5), with the same plasma parameters is employed a lower beam current (I_{Beam}=0.31 MA) results. This is due to the loss of particles through the ends of the FRC, which is very important in this case.

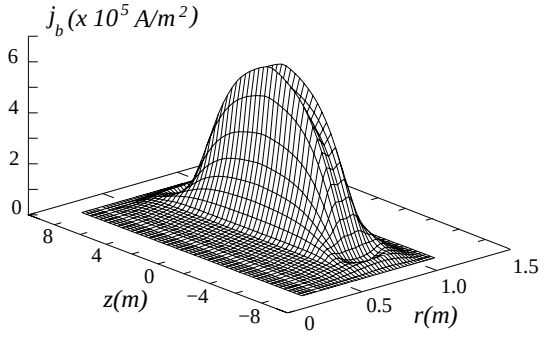

Fig. 6. Beam current density for peaked equilibrium.

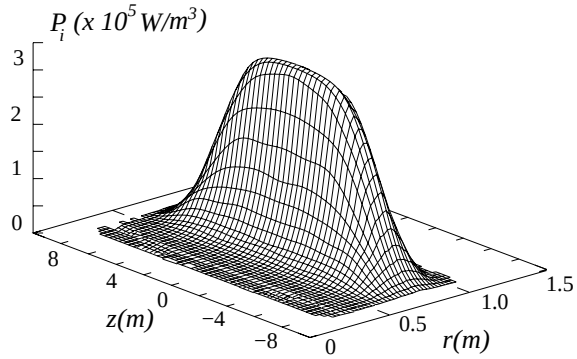

Fig. 7. Deposited beam power for peaked equilibrium.

Since the total beam current obtained for peaked and hollow equilibria is much lower than the value quoted in [7] we calculate below the maximum current that could be driven by the beam and discuss the effects that reduce it.

The distance traveled by a beam ion in a field free plasma with uniform density until it thermalizes can be calculated as:

$$L = \int_{u_i}^{u_{th}} \frac{u}{(du/dt)} du ,$$

where u_i is the initial ion velocity, $du/dt = -\nu_s u$ [10] and the slowing down collision frequency, ν_s, must contain the contribution of the three plasma species. The maximum current that could be driven by the beam can be estimated by dividing L by the length of the ion orbit, which is approximately $2\pi r_0$. Using the parameters proposed in [7] we obtained an amplification factor ($L/2\pi r_0$) of 2.7×10^5, corresponding to a total current of 1.35 MA for a 5 A beam. This is substantially smaller than the value quoted in [7], where it is assumed that 5 A of neutral beam current would produce 8 MA of plasma current. A substantially larger, but incorrect, amplification factor is obtained calculating the distance traveled by the ions as: L=u_i/ν_0, where ν_0 is the collision frequency calculated with u_i.

The current calculated with the code depends on the type of equilibrium considered (higher for peaked than for hollow) but it is always lower than the 1.35 MA indicated above. Since basically all the neutral beam particles get ionized there are two effects that reduce the beam current:

a) A fraction of the ionized particles, approximately 18% for peaked and 62% for hollow equilibria, is lost through the ends of the configuration before becoming thermalized. These losses could be reduced adding magnetic mirrors.
b) Due to the particular magnetic field structure of FRCs, particles ionized close to the separatrix end up rotating around the FRC axis in the counter-current sense.

Figure 8 shows the orbits of two particles which were ionized at different distance from the FRC axis. Particle 1 rotates in the "positive" (current) sense, thus contributing to the plasma current while particle 2 rotates in the "negative" sense, reducing the plasma current. For the parameters proposed in [7] there are more particles rotating in the negative sense (N_{pos}/N_{neg}=0.88 for the peaked equilibrium used in Fig. 6) but their azimuthal velocity is generally smaller than that of the particles rotating in the positive sense and a positive beam current results ($|I_{pos}/I_{neg}|$=6.6).

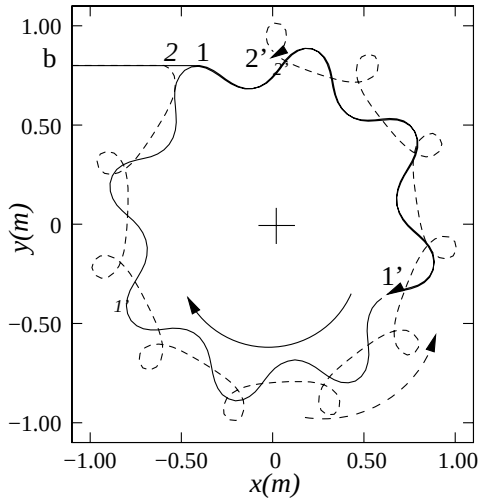

Fig. 8. Particle orbits for different ionization positions.

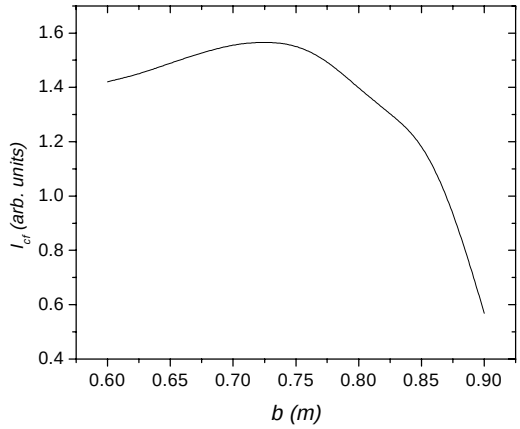

Fig. 9. Collisionless plasma current as a function of impact parameter.

The probability that particles become ionized at a given location and the amount of current produced by these particles depend upon the plasma and beam parameters. To find the impact parameter that results in the highest efficiency we removed the collisions from the code (to speed up the computation) and calculated the current produced in a fixed time for different values of *b*. A fixed time is needed because in the collisionless case particles do not became thermalized. The assumption here is that restoring collisions would not change the value of *b* that results in the highest efficiency. We show, in Fig. 9, the current produced for different impact parameters in the absence of collisions. The highest current is obtained for $b \approx 0.725$, smaller than the null radius.

In the low beam current regime considered here the beam plasma current increases linearly with the neutral current and with the energy of the neutral particles. Since the current produced with the plasma parameters proposed in [7] is very small, we tried to find a set of parameters, not too different from the original ones, that would result in higher current drive efficiencies. With E_{Beam}=1.2 MeV, r_s=106 cm, B_{ext}=6.4 T, T_e=T_D=T_{He}=87.5 keV ($n_{e,\max}$=6.4×10^{14} cm^{-3}) and a peaked equilibrium we obtained a total beam current of I_{Beam}=1.26 MA (for a 5 A beam). With these parameters, driving 8 MA of beam current would require approximately 32 A of NB current and an injected power of about 38 MW.

Formation and sustainment of a flux core spheromak by DC helicity injection

The Versatile Advection Code (VAC) [11] is being employed to study the formation of a flux core spheromak (FCS) and its sustainment by DC helicity injection. The code is fully 3D (no Fourier decomposition) and solves the 3D resistive isothermal MHD equations using a finite volume method. Fluxes are computed with a MUSCL TVD method and Roe's approximate Riemann solver. Initial studies, with fixed density (zero beta limit), are aimed at testing the capability of the code to follow the evolution of an unstable screw pinch until the FCS is formed and the effect of different boundary conditions. The geometry and grid employed, which is uniform in the axial direction, are shown in Fig. 10. The FCS is formed inside a cilindrical flux conserver in the presence of an external axial field. Figure 11 presents a sequence of poloidal flux contours showing the initial screw pinch and the final FCS.

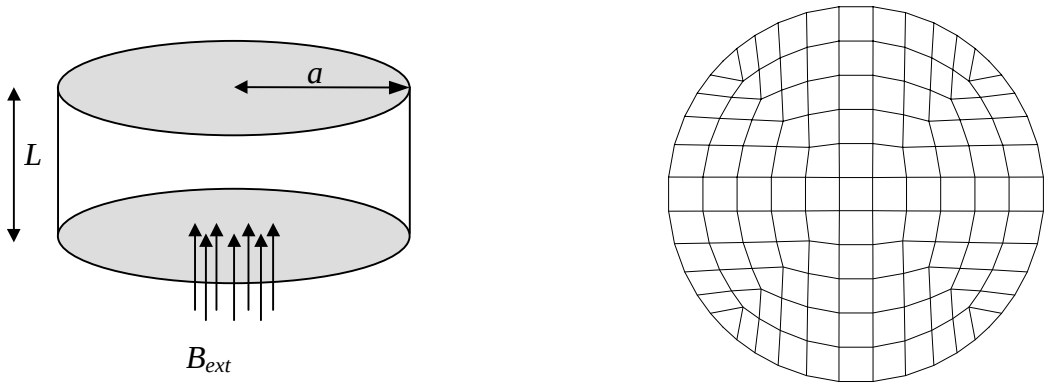

Fig. 10. Geometry and grid employed in the computations.

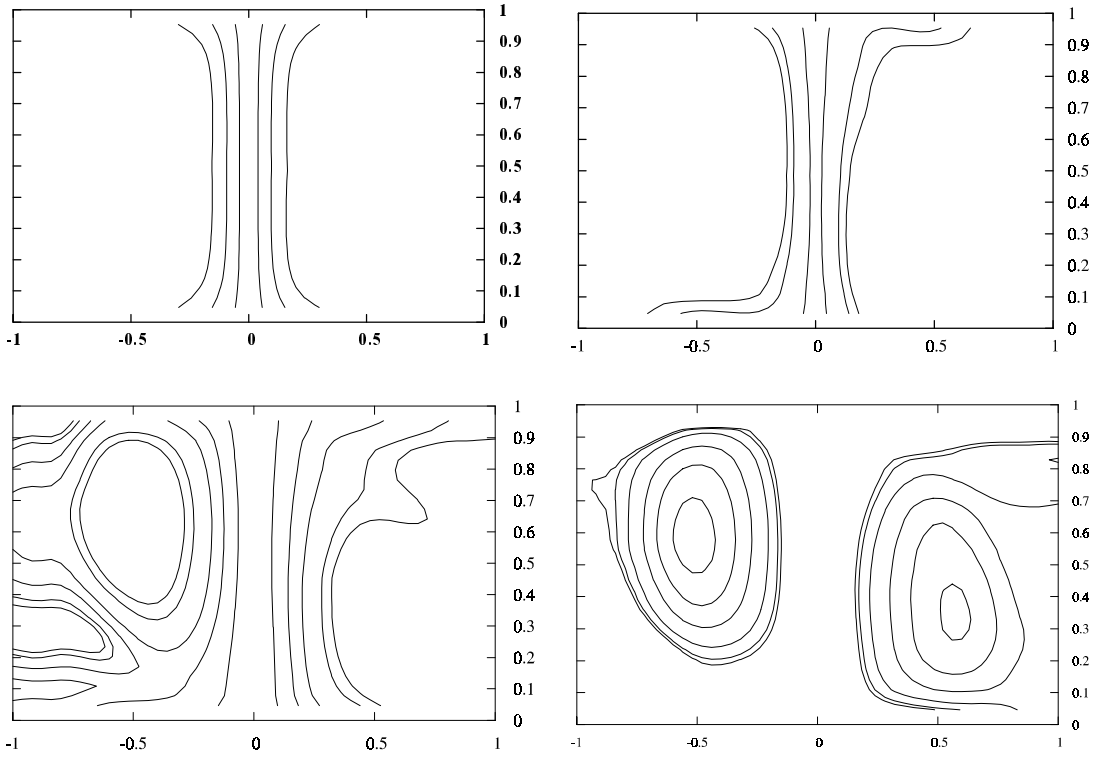

Fig. 11. Sequence of contour plots showing the formation of a spheromak

References

[1] R. Farengo and R. A. Clemente, *Phys. Plasmas* **13,** 042515 (2006).
[2] I. R. Jones and W. Hugrass, *J. Plasma Phys.* **26**, 441 (1981).
[3] G. A. Collins et al. *Nucl. Fusion* **28**, 255 (1988).
[4] W. K. Bertram, *Plasma Phys. Controlled Fusion* **30**, 425 (1987).
[5] R. A. Clemente and R. Farengo, *Braz. J. Phys.* **33**, 867 (2003).
[6] H. E. Ferrari, R. Farengo and R. A. Clemente, *Phys. Plasmas* **13,** 032505 (2006).
[7] H. Momota et al., *Fusion Technol.* **21**, 2307 (1992).
[8] A. F. Lifschitz, R. Farengo and N. R. Arista, *Nucl. Fusion* **42**, 863 (2002). A. F. Lifschitz, R. Farengo and A. L. Hoffman *Nucl. Fusion* **44**, 1015 (2004).
[9] A. F. Lifschitz, R. Farengo and N. R. Arista, *Plasma Phys. Control. Fusion* **44**, 1979 (2002).
[10] J. D. Huba, in "NRL Plasma Formulary", Office of Naval Research, USA (1998), pag. 31.
[11] See http://www.phys.uu.nl/~toth/ .